International Journal of Electrical and Computer Engineering (IJECE)
Vol. 11, No. 4, August 2021, pp. 2876~2888
ISSN: 2088-8708, DOI: 10.11591/ijece.v11i4.pp2876-2888

Fuzzy logic power management for a PV/wind microgrid with backup and storage systems

Aysar M. Yasin, Mohammed F. Alsayed
Faculty of Engineering, Energy Engineering and Environment Department, An-Najah National University, Nablus-Palestine

Article Info

Article history:

Received Sep 13, 2020
Revised Oct 14, 2020
Accepted Dec 12, 2020

Keywords:

Distributed generation
Energy management
Microgrid
Fuzzy logic controller
Renewable energy sources
SuperCapacitor

ABSTRACT

This work introduces a power management scheme based on the fuzzy logic controller (FLC) to manage the power flows in a small and local distributed generation system. The stand-alone microgrid (MG) includes wind and PV generators as main power sources. The backup system includes a battery storage system (BSS) and a diesel generator (DG) combined with a supercapacitor (SC). The different energy sources are interconnected through the DC bus. The MG is modeled using MATLAB/Simulink Sim_Power System™. The SC is used to compensate for the shortage of power during the start-up of the DG and to compensate for the limits on the charging/discharging current of the BSS. The power balance of the system is the chief objective of the proposed management scheme. Some performance indexes are evaluated: the frequency-deviation, the stability of the DC bus voltage, and the AC voltage total harmonic distortion. The performance of the planned scheme is assessed by two 24-hours simulation sets. Simulation results confirm the effectiveness of FLC-based management. Moreover, the effectiveness of the FLC approach is compared with the deterministic approach. FLC approach has saved 18.7% from the daily load over the deterministic approach. The study shows that the quality of the power signal in the case of FLC is better than the deterministic approach.

Corresponding Author:

Aysar M. Yasin
Energy Engineering and Environment Department
An-Najah National University
Omar Ibn Al-Khattab St., PO Box 7, Nablus, Nablus, Palestine
Email: aysar.yasin@najah.edu

1. INTRODUCTION

The microgrid (MG) under investigation in this study is off-grid and all power sources are connected through a DC bus as shown in Figure 1. This configuration makes the integration of RES easier, more effective, and is considered a remarkable solution for off-grid power systems [1]. The quality of the power signal must be within an accepted range. Steady supply voltage and AC frequency, lower total harmonic distortion of the voltage signal (THDv) [2]. The MG in this study primarily includes wind energy (WEG) and PV energy generators (PVEG). For maximum utilization of the attainable energy battery storage system (BSS) is used as primary energy storage, it keeps DC-bus voltage within the rated range in case of unexpected load deviations. The diesel generator (DG) joined with Supercapacitor (SC) is used as a secondary backup. The system must be suitably controlled to achieve high efficiency and a better balance of load supply. The DG is a consistent backup energy source and can provide durable backing, it is commonly used in stand-alone MG power systems [3]. Its output voltage and frequency take a few seconds to reach stability due to slow dynamic behavior [4]. SC will provide energy compensation during the starting up of

DG. It supplies energy in electrical form, has a fast response, and is capable to fast accommodate large amounts of energy [5].

This research considers a stand-alone DC MG based on WEG, PVEG, BSS, and DG combined with SC. It is modeled and controlled using MATLAB/Simulink Sim_Power System™. It proposed an energy management strategy to supply the load with the least loss of power supply. The DC bus is regulated within the accepted range (380-400 V) under different weather conditions and various load demands. More precisely, voltage-regulation, power-sharing, and energy storage management should be confirmed [6]. For this purpose, a management system unit is required to control the main components based on the power generated from WEG and PVEG, the BSS state of charge (SoC), and SC.

Building and applying a conventional management approach for such a complicated system is not easy. It encounters low dynamic performance, higher steady-state error. The switching losses of the power converters and high fault-tolerant negatively affect the THD of the output voltage signal. The management strategy needs flexibility and fast reactions. So, a fuzzy logic controller (FLC) approach is suggested in this paper. FL is a mathematical system that evaluates analog input values in terms of logical variables that take on continuous values between 0 and 1, contrary to classical or digital logic, which works on discrete values of either 1 or 0 [7]. It is very suitable for controlling systems with high complexity whose behaviors are not well understood, and/or in situations where a fast approximate solution is warranted [8]. FLC can play a significant role because knowledge-based design rules can straightforwardly be realized in systems with unknown structures. The proposed control algorithm confirms an optimal operating system at different climatic conditions, it proposed an ideal solution for operating the standalone application. The proposed control algorithm ensures effective transferring of all produced power from PVEG and WEG, reduces dependency on DG, ensures continuous charging and discharging of the BSS.

References from [9-23] discussed the energy management of MG based on RES. In [9], a supervisor energy management strategy based on FLC of hybrid WEG/PVEG/DG with BSS is implemented. In [10], FLC is utilized to achieve a standalone DC MG based on PVEG/SC energy flow balance. The SC is used for unexpected power demand while BSS is used for the long-term period. In [11], an MG mainly consisted of PVEG, and SOFC is considered. An optimization method is proposed based on FLC to optimize energy flow between MG and SC. The control strategy ensures smooth dynamic response and stability. The output power signal is assessed using THD, it is found within the IEEE recommended range. In [12], and energy management algorithm based on FLC is designed for residential on-grid MG based on RES and ESS. The objective of the design is to control the power quality of the grid and reduce fluctuations. The study used the MG energy rate of change and the SOC of the BSS to maintain the power delivered or absorbed by the grid. In [13], and energy management strategy based on FLC is designed for supplying a residential load with PV-grid connected system and BSS. The strategy is implemented to manage the residential energy demand based on load priority. In [14], a PVEG with BSS is attached with an FLC system to cover the demands of a residential DC load, it adjusts the power conditioner to control the power flow from/to BSS. Results show the preferences of FLC over the conventional PID controller. In [15], and FLC is utilized to manage a PVEG standalone MG system. FC and BSS are included to ensure a reliable power supply. The management strategy optimizes the proposed power generation and maximizes the production of hydrogen. In [16], FLC based energy management scheme is utilized to optimize the energy generated from PVEG and FC to fulfill a water pumping load. The storage system is mechanical and electrochemical. The controller assurances uninterrupted power production and water availability with the least cost. In [17], A FLC scheme is implemented to manage the power flow of a PVEG/WEG/BSS standalone MG. The main objective of the scheme is to balance power generation and the load despite its fluctuations. Simulation results validate the approach capability.

In [18], an FLC energy management system was developed for the multi-operation mode of smart MG. The residential MG consists of PVEG, FC, and BSS. The control scheme is designed to choose the suitable procedure style considering both real and long-term forecast data of the energy generation and consumption. Energy distribution and energy cost analysis are accomplished for each scenario to confirm the control scheme. In [19], the optimal design of FLC is performed to manage the power flow from different RES. Various storage systems including BSS, SC, and hydrogen storage tanks were considered to overcome RES generation fluctuations. [20] Utilized the FLC energy management approach to lessen the unsystematic and irregular nature of RES to the MG system. The MG simulation model mainly includes PV systems and BSS units. The MG under diverse working styles in addition to the PV system are empowered through harmonized control of the bidirectional DC/AC converter and the BSS unit. In [21] a smart BSS management strategy is proposed for MG consisted of PVEG, BSS, and a small suburban group. The case study is located in high solar radiation potential but suffering from the frequent movement of the clouds. The management strategy is built using FLC that defines the rules based on the behavior of the residents, energy from PVEG, SOC of BSS, in addition to the price of the kWh purchased from the distribution company. The strategy

succeeded to supply electric power to houses without disturbance to the grid and maintaining the SOC of BSS at maximum. In [22] two FLCs were used to manage the energy generated from PVEG, WEG, FC, DG, and BSS. MATLAB/Simulink is utilized for simulating the MG RES. Results show that intermittency in RES can be controlled by FLCs to offer uninterrupted power. In [23] a balance in power flow from different energy sources is preserved by the aid of FLC. A small number of rules is used to keep continuous, decreasing the use of BSS; and observing a balance between power sources, storage, and load.

This paper comes with the following contributions and enhancements: Energy management strategy based on FLC approach for a stand-alone DC MG is realized. The scheme is based on matching DC-bus voltage using WEG/PVEG/load's sharing and PID controllers. The DG is utilized as a backup if BSS is discharged. The scheme considers the slow dynamic of DG during starting up by utilizing SC. This work utilizes SC also for discharging/charging energy when the deficient/excess power is greater than the capacity of BSS. This strategy considers the problem of the fast self-discharging problem of SC. A dump load is considered in the system to effectively manage the excess power in the case of fully charged BSS and SC. This work solved the low dynamic performance encountered in the deterministic approach, reduce steady-state error, and switching losses of the power converters. It also reduces THDv of the output voltage signal.

2. RESEARCH METHOD AND SYSTEM CONFIGURATION

The research method followed in this study is mainly based on simulation analysis using MATLAB/Simulink Sim_Power System™ software. Figure 1 shows the schematic diagram of the considered DC microgrid power plant. The main elements are WEG, PVG, BSS, SC, and DG. Each component is modeled and validated. The management strategy is built using the FLC approach. The main objective is to maintain an effective power balance from the different sources at the same time preserve high power quality. Different simulation sets were performed at different load and weather conditions. Various technical indicators were defined.

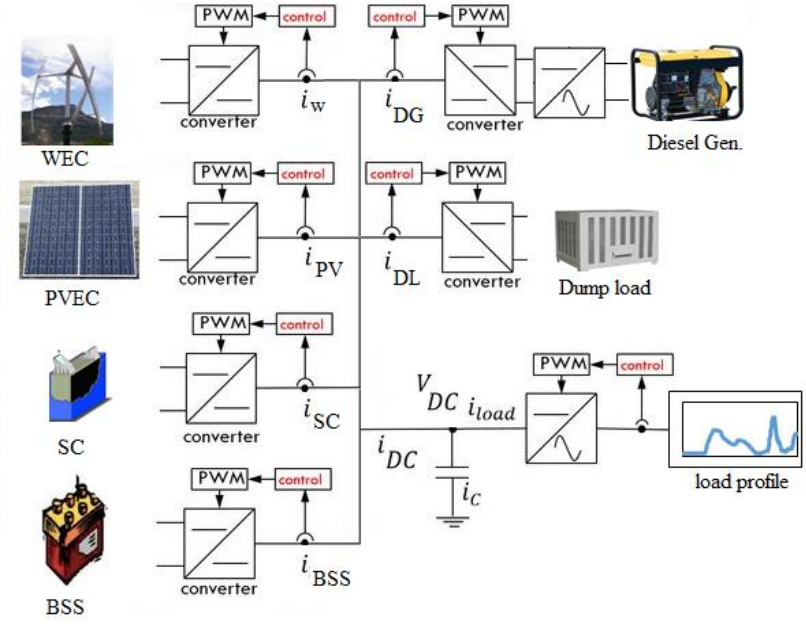

Figure 1. Representation of the standalone power system

2.1. PVEG system

The PV cell model used in this study depends on one-diode with four parameters as shown in Figure 2. In (1) to (6) are modeling the PV modules used in this study [24].

$$I = I_L - I_o[\exp(V + Rs\, I/V_t a) - 1] \quad (1)$$

$$V_t = N_s kT/q \quad (2)$$

$$I = I_o \exp(V_{oc}/N_s V_t) \quad (3)$$

$$V_{oc}(T) = V_{oc+} k_v \ (T_{cell} - T_{stc}) \quad (4)$$

$$I_{sc}(T) = I_{sc} \ (1 + \frac{k_i}{100}(T_{cell} - T_{stc})) \quad (5)$$

$$T_{cell} = T_{ambient} - \frac{NOCT-20}{0.8} G \quad (6)$$

Where a is the ideality-factor, I is operation current, I_L is light-current, I_0 is diode reverse saturation-current, k is Boltzmann's constant (J/°K), Kv is the voltage coefficient temperature, V/°C. ki is the current-coefficient temperature, A/°C, Ns is the number of cells in the panel connected in series, q is electron's charge, Rs is the equivalent series resistance of the array, T is PV cell temperature at STC (°K), V is operation voltage of the array and Vt is the thermal voltage of the array. T_{cell} is the cell temperature and NOCT is the nominal operating conditions temperature. The model is validated as shown in Figure 3. PVEG is annexed with observation algorithms (P&O) MPPT controller [25]. The topology of the control system and its validation is shown in Figure 4. The total power rating of the PV system is 1.88 kWp.

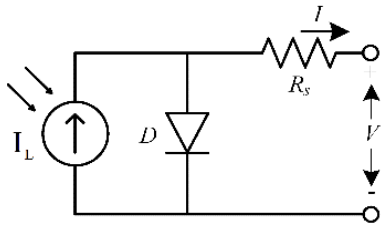

Figure 2. One-diode PV cell equivalent circuit model

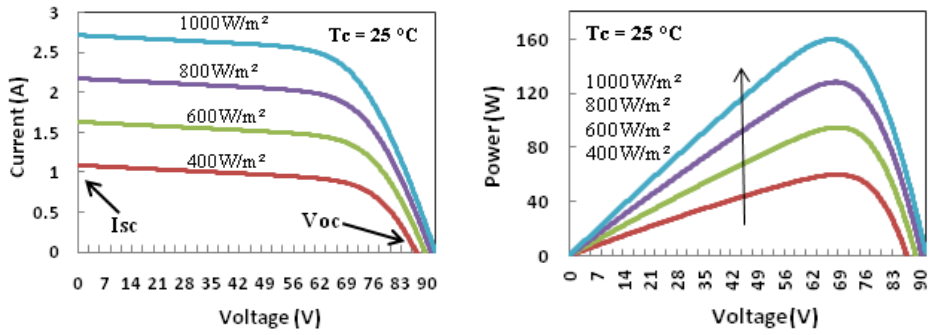

Figure 3. I-V characteristics of the solar array model at different solar radiation and 25 °C cell temperature

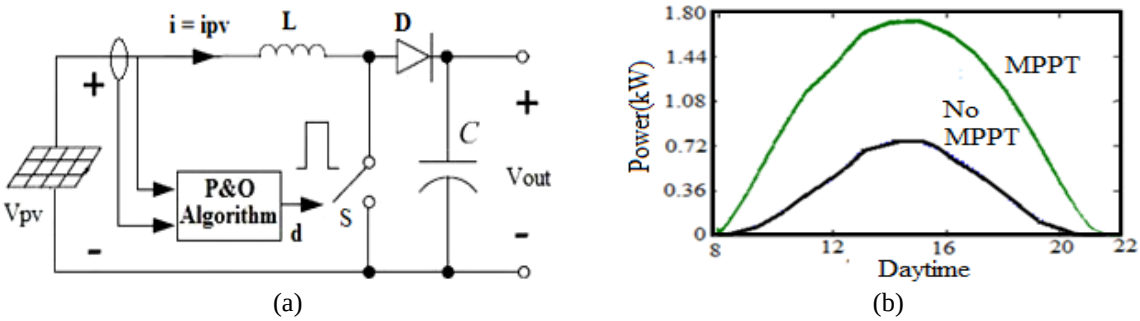

(a) (b)

Figure 4. DC/DC boost-converter controlled by (a) MPPT control scheme, and (b) its validation

2.2. WEG system

A vertical axis micro wind turbine with three helical blades has been modeled. The wind turbine is fitted with a permanent magnet synchronous generator (PMSG). The mathematical model of the WEG system is illustrated in (7) through (9). The power generated from the rotor turbine wind is given by (7) [26, 27].

$$P_t = \frac{1}{2}\rho a\, C_p\, A_t\, V_w{}^3 \tag{7}$$

Where At is swept area of the turbine, Cp is wind power coefficient, **ρ**a is air density and V_w is wind velocity. The power coefficient (Cp) curve is shown in Figure 5. The wind turbine torque (Tt) on the shaft can be calculated from the wind power as in (8), in which the rotational speed of the blades Ω is measured from the mechanical model of the PMSG.

$$T_t = P_t/\Omega = \frac{1}{2}\rho a C_p A_t\, V_w^3/\Omega \tag{8}$$

The generated shaft mechanical torque (Tt) is used as an input mechanical power to an electrical generator. The mechanical system of the electrical generator is represented by (9) [28].

$$\frac{d}{dt}w_r = \frac{1}{J}(T_e - Fw_r - T_t) \tag{9}$$

Where F is combined viscous friction of rotor and load, Te: electromagnetic torque, J has combined inertia of rotor and load and ωr is the angular velocity. Te is calculated using the sinusoidal electrical model in the synchronous reference frame [29]. Figure 6 shows the schematic diagram of the WEG model and its validation.

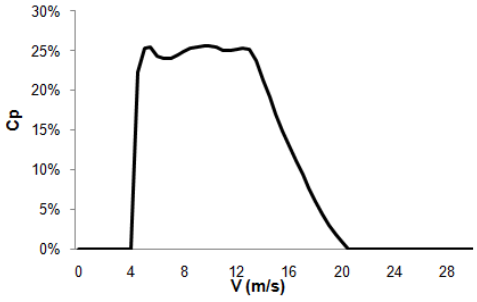

Figure 5. Power coefficient vs different wind speeds

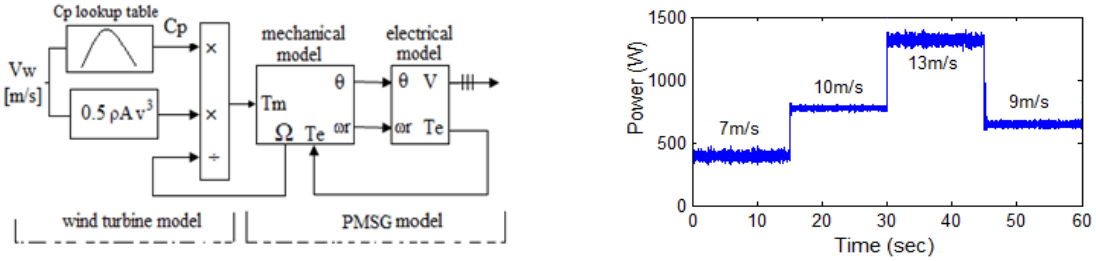

(a) (b)

Figure 6. Schematic of the Simulink SimPowSys model of (a) WEG model, and (b) its validation

2.3. Diesel generator (GD)

The DG's basic components are the engine, governor, excitation, and synchronous generator. The DG model mainly consists of engine speed control, synchronous generator, and voltage regulator. A

schematic of the DG module is shown in Figure 7(a) [29] and The MATLAB/Simulink SimPowSys™ simulation model is shown in Figure 7(b). The mechanical aspect is defined by the combustion process and engine model while the electrical aspect is defined by the synchronous generator and voltage regulation. The model uses tabulated mechanical power data concerning rotational speed (rad/s) to estimate output mechanical power [30]. The automatic voltage regulator (AVR) is responsible for regulating the excitation voltage of the synchronous generator, it controls the rotor angle and the generator terminal voltage to obtain a good dynamic system and improves the stability.

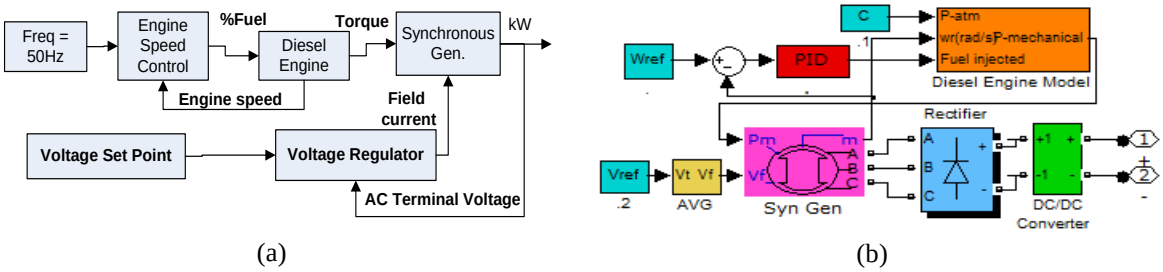

(a) (b)

Figure 7. Modeling of DG: (a) Schematic of DG model, and (b) MATLAB/SimPowSys simulation model

2.4. Battery storage system (BSS)

The built-in SimPowerSys™ [31] block model of a lead-acid BSS is considered in this simulation study, it mainly consisted of a controlled voltage source that is a function of battery charging and discharging current and battery capacity. The model is shown in Figure 8(a). The battery is attached to the DC bus via boost/buck DC/DC converter. The schematic of the control strategy is shown in Figure 8(b).

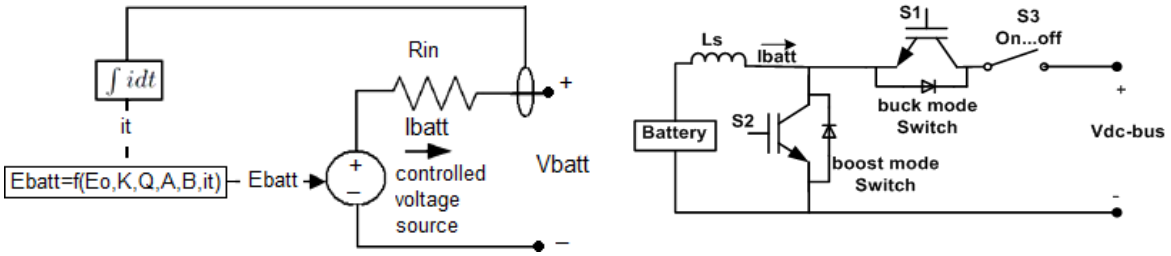

(a) (b)

Figure 8. Modeling and control of battery storage system: (a) The equivalent electrical circuit of the lead acid BSS, and (b) The schematic of the control strategy of the battery and DC bus

A constant resistance is assumed during the different modes of battery. The controlled source is described using (10) and (11) [31].

$$E_{batt} = E_0 - K\frac{Q}{Q-it} + Ae^{-B.it} \quad (10)$$

$$V_{batt} = E_{batt} - R_{in} . I_{batt} \quad (11)$$

The SoC-BSS is estimated using the (12).

$$SoC\_BSS = 1 - \frac{1}{Q}\int_0^t I_{batt}\, dt \quad (12)$$

Where A is the exponential zone amplitude, B is the exponential zone time constant inverse, Ebatt is no-load voltage, is E_0 is battery constant voltage, I_{batt} is battery charging and discharging current, K is polarisation voltage, Q is battery capacity, it is extracted capacity, R_{in} is the internal resistance of the battery, and Vbatt is the terminal voltage of the battery.

2.5. Super-capacitor SC

The SC is modeled as internal resistance and a controlled voltage source as shown in Figure 9(a) [31]. Figure 9(b) shows the performance of the SC model during charging and self-discharging. The supercapacitor output voltage Vsc, supercapacitor current i_{sc}, and self-discharge current i_{self_dis} are expressed using (13) through (15).

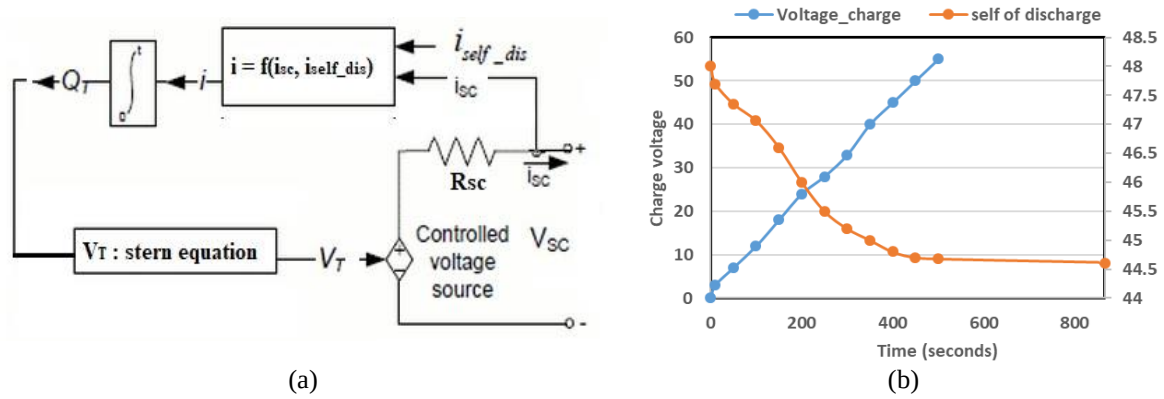

(a) (b)

Figure 9. Modeling and validation of super-capacitor SC: (a) Equivalent electrical circuit of SC, and (b) its performance during charging and self-discharging

$$V_{sc} = V_T - i_{sc} * R_{sc} \quad (13)$$

$$Q_T = \int_0^t i_{sc}\, dt \quad (14)$$

$$Q_T = \int_0^t i_{self\_dis}\, dt \;@\; i_{sc} = 0 \quad (15)$$

Where V_T is the stern equation which is a function of the number of parallel and series supercapacitor, electric charge Q_T, the permittivity of a material, operating temperature, number of electrode layers, Interfacial area between electrodes and electrolytes [31]. The model is built based on the Stern model as explained and validated in [32]. The SoC-SC of the supercapacitor is calculated using the (16).

$$SoC_{SC} = \frac{Q_{initial} - \int_0^t i(t)dt}{Q_t} \quad (16)$$

Where $Q_{initial}$ is the initial amount of supercapacitor electric charge and i(t) is a function of supercapacitor current and self-discharge current. The rated capacitance of the supercapacitor is 99.5 F and the rated voltage is 48 V.

2.5. Dump load (DL)

The DL consists of a power converter and a bank of resistors. The DL-rated power is selected to be 28% larger than PVEG and WEG rated output power. The DL is connected to the DC bus [33].

3. FUZZY LOGIC ENERGY MANAGEMENT (FEM)

Each fuzzy logic system is composed of rules, fuzzifier, inference, and defuzzifier as shown in Figure 10(a). The FLC model consisted of fuzzy inputs of SoC of SC and BSS in addition to control current of BSS. The inputs are entered into an inference block that includes the rules. The main components of each FLC are shown in Figure 10(b). The fuzzy input sets and rules are entered into the inference block. The rules are derived from human experience. The interesting thing is that numerical data obtained from measurement or sensors and linguistic information obtained from human experience are utilized to form a fuzzy rule. Fuzzy inference expresses the input to an output using fuzzy logic. In this study, the fuzzy inference is built using Mamdani-type [34]. The aggregate output fuzzy set is entered into the defuzzification process. The output is a single number. Though, the aggregate of a fuzzy set includes a variety of output values, and so

must be defuzzified to decide a single output value from the set. The centroid which calculates the center of the area under the curve is used in this study. The main objective of FEM is to ensure the continuity of power flow to the load. The FEM operates in excess and deficit power modes. The excess mode has occurred when the energy generated from RES is greater than the required power from the load while the deficit mode has occurred when generated power is less than load power. The controlling current is estimated by the control strategy based on the Pnet, thus it indicates the working mode. In the case of excess power, the surplus energy will be directed into the storage system or to DL in case of the storage system is full. In the case of deficit power, the shortage will be covered by a storage system or DG. The control strategy depends primarily on three inputs data: The controlling current of BSS (i_{BSS}), the state of charge of the BSS (SoC-_BSS), and the state of charge of SCs (SoC_SC).

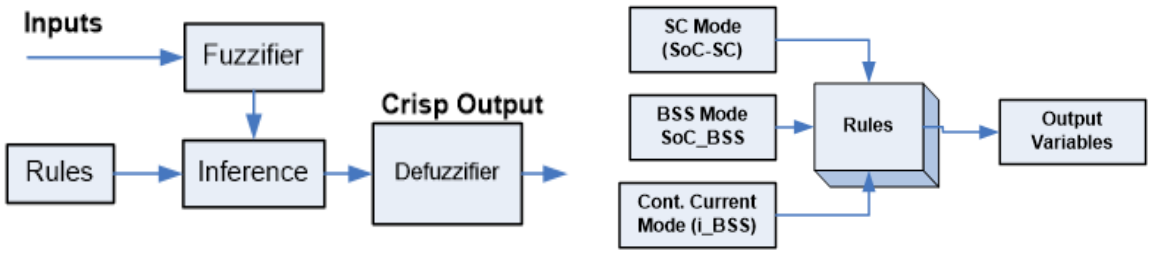

Figure 10. Fuzzy logic control system: (a) Main components of FLC, and (b) common configuration of the FLC model

3.1. Fuzzification

The FEM has three fuzzy inputs and one fuzzy output as shown in Figure 11. The three inputs are i_{BSS}SoC_BSS, and SoC_SC. The SoC_BSS and SoC_SC are VL, L, M, H, and VH which stands for very low, low, medium, high, and very, respectively. The i_{BSS} is HD, D, LD, LE, E, and HE which stands for the high deficit, deficit, low deficit, low excess, excess, and high excess, respectively.

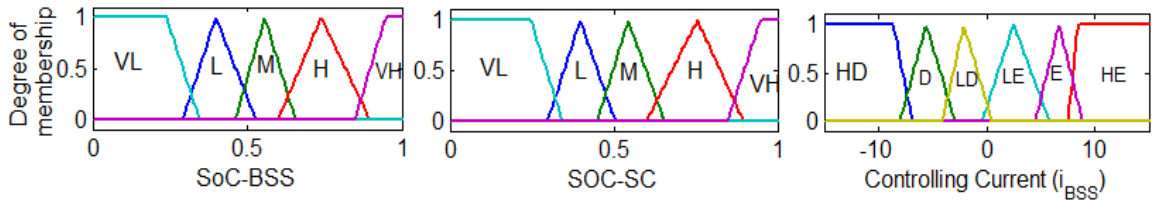

Figure 11. Membership-functions of the inputs SOC-BSS, SOC-SC, and controlling current

3.2. Inference

Table 1 indicates the fuzzy-rules for the FEM depending on the power mode. Two modes are depicted, the excess power mode, and the deficit power mode. The outputs of the fuzzy inference system (FIS) are the probability P(t) to select certain mode: (CS) charging SC, (CB) charging BSS, (CS+CB) charging BSS and CS, (CB+DL) charging BSS, and dump load, (DL) charge DL, (DB) discharge BSS, (DS+DB) discharge SC and BSS, (DG) turn on the DG, and (LL) limit load. In the next step, the If-Then logic inference is defined. An explanation example is introduced to one of the cases that may occur at low excess mode: *IF the power mode is at HD AND SOC_BSS is VL AND SOC_SC is M THEN the probability to make DG works is High.*

3.3. Defuzzification

The next step after applying the rules that correspond to the fuzzification, the defuzzification is defined. In this study, the method of the center of gravity is used. Figure 12 shows the output membership functions of the FEM system which contains sigmoid-functions with different values for each category.

Table 1. Fuzzy-inference of fuzzy-inputs

Power Mode		SoC_BSS		SoC_SC		Action
HD OR D	AND	VL OR L OR M OR H OR VH	AND	VL OR L	THEN	LL
HD	AND	VL OR L OR M	AND	M OR H OR VH	THEN	DG
		H OR VH		M OR H OR VH		DS+DB
	AND	VL OR L	AND	M OR H OR VH	THEN	DG
D		M OR H OR VH		M OR H OR VH		DS+DB
	AND	VL OR L	AND	VL OR L		LL
LD		M OR H OR VH		VL OR L OR M OR H OR VH	THEN	DB
		VL OR L		M OR H OR VH		DG
	AND	VL OR L OR M OR H OR VH	AND	VL OR L OR M		CS
		VL OR L OR M		H OR VH		CB
LE		H OR VH		H	THEN	CS
		H OR VH		VH		DL
E OR HE	AND	VL OR L OR M OR H	AND	VL OR L OR M OR H		CS+CB
	AND	VH	AND	VL OR L OR M OR H		CS
E		VL OR L OR M		VH	THEN	CB
		VH		VH		DL
		H		VH		CB+DL
		VL OR L OR M OR H		VH		CB+DL
HE	AND	VH	AND	VL OR L OR M	THEN	CS
		VH		H OR VH		DL

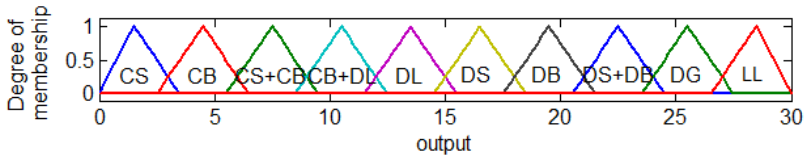

Figure 12. Membership-functions of the output-variable for each element in the complex hybrid power system

4. SIMULATION RESULTS AND DISCUSSION

The simulation model of the MG under investigation is built using the MATLAB/Simulink Sim_Power environment. The converters are controlled using the proposed PID controller energy management control strategy, which aims to keep the DC-bus within a predefined accepted range and balance the power flow. The objective of the simulation tests is to confirm the effectiveness of the proposed energy management strategy using well-defined performance indexes; the frequency deviation, the stability of the DC bus voltage, and the THDv. In addition to that, the effective distribution of the required energy to the different power sources is another indicator of the effectiveness of energy management strategy.

For performing the required analysis, simulation results were monitored and recorded, these outputs include generated power from PVEG, WEG, and DG. The energy is injected or extracted from BSS and SC systems. The SoC-BSS and SoC-SC as well. The charging i_{CBSS} and discharging i_{DBSS} controlling the current of BSS are also estimated. It is worth mentioning that the simulation is based on real weather data and load demand for a specific location. The solar radiation and load demand are expressed per unit (pu) at a base value of 1 kW/m^2. The wind speed and temperature are expressed in m/s and ^{o}C, respectively. The time duration of the simulation set is 24 hours (86400 seconds). Figure 13 shows the annual average weather data and load profile applied to all simulation cases. Figure 13 simulates the event of changeover mode resulted from sudden cloud effect on PVEG, sudden wind drop effect on WEG, DG set takeover, and the energy dip to load situation. This is very important as it directly affects THD.

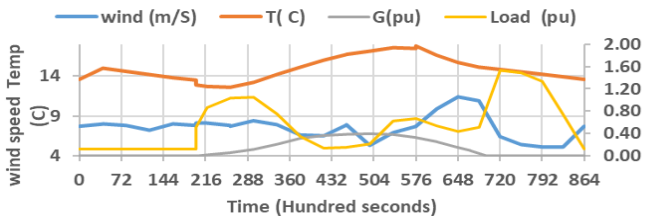

Figure 13. The annual average weather data and load profile applied during simulation set 1 and set 2

4.1. Simulation set 1

The simulation set is divided into 4 periods and the SoC-BSS and SoC_SC are assigned to 0.6. The renewable energy generated from PVEG and WEG is based on the data. The corresponding energy generated from PVEG and WEG is illustrated in Figure 14(a). The power injected from DG is zero all over the simulation period. The SoC_BSS, SoC_SC, and the BSS controlling current i_BSS clearly show the working mode of the BSS and SC.

Surplus energy is generated in the interval from 0:00-6:00 AM. From 6:00 AM-9:45 AM, a deficiency in generated energy has occurred and compensated from BSS and SC. From 9:45 AM-7:25 PM surplus energy is generated and injected into BSS and SC. From 7:25 PM-12:00 PM, a power generation deficiency has occurred and compensated from BSS and SC. Details are illustrated in Figures 14(b) and (c). The frequency deviation, THDv in addition to the normalized DC bus voltage are investigated in this study. The THDv did not exceed the 4% threshold limit. The frequency deviation and the normalized DC bus voltage are within the accepted range. Details are illustrated in Figure 14(d).

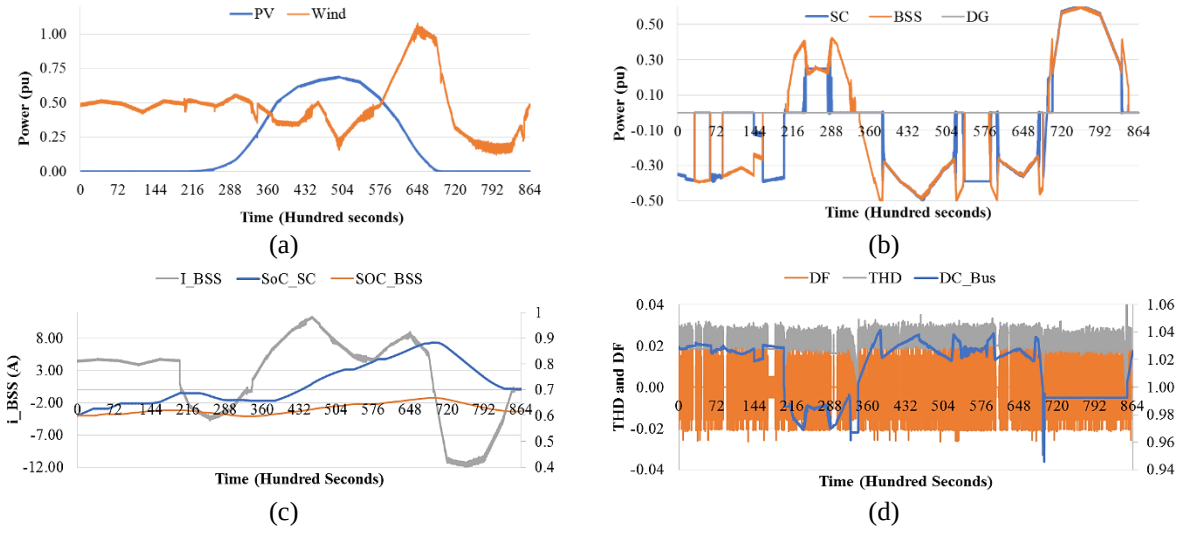

Figure 14. Results of simulation set 1 (a) Power output from PVEG and WEG, (b) Injected/absorbed power from BSS and SC, (c) The SoC_BSS, SoC_SC, and (d) Controlling current i_BSS, THDv, and Δf in addition to the normalized DC-bus voltage

4.2. Simulation set 2

Compared to simulation set 1, the metrological data and load demand are kept constant. The corresponding energy from PVEG and WEG are identical to simulation set 1. Details are shown in Figure 14(a). Simulation set 2 assumed that SoC-BSS and SoC_SC are equal to 0.4. The power-sharing among the power produced from PVEG, WEG, load demand, BSS, and SC, generated DG power are illustrated in detail in this study. Details are shown in Figure 15(a). The charge/discharge mode of the BSS under different circumstances of PVEG and WEG produced power and load variation is illustrated in this study. Details are shown in Figure 15(b). The simulation study shows that the quality of the power signal is high. Details are shown in Figure 15(c). Once again, the simulation results of set 2 shown in Figure 15 confirms the applicability of the control strategy.

To show up the advantageous features of FLC over the deterministic approach, a simulation comparison study is implemented. The study is based on data other than used in simulation sets 1 and 2. Details of the data are shown in Figure 16(a). The average daily load is 10.67 kWh. The comparison is based on the amount of energy flow from/to the energy storage system, energy injected to DL, and the energy generated from DG. A better management approach ensures higher energy injection to the storage system, less energy injection to DL, and lower dependency on DG. The system components, capacities, and constraints are identical to ensure a fair comparison. The control approach has a great effect on the charging/discharging mode of the BSS and SC. This mainly affects the amount of energy injected into DL and the operating hours of DG. The amount of energy injected into DL is zero in the case of the FLC approach, while it is not in the case of a deterministic approach. This is considered a drawback of the deterministic approach.

The energy generated from DG is zero for both deterministic and fuzzy approaches. This is illustrated in Figure 16(b). The SoC of SC and BSS is a good indicator of the amount of energy injected/delivered to the storage system. The SoC of BSS and SC at fuzzy and deterministic approaches are studied in the comparison set study. The SoC analysis study shows that the SoC of BSS at the fuzzy approach increases from 0.6 to 0.67 while it keeps 0.6 in the deterministic approach. Energy-wise the difference is equal to 2.5 kWh/day. In the same context, SoC of SC increased from 0.6 to 0.81 and from 0.6 to 0.84 for the fuzzy approach and deterministic approach, respectively. Energy-wise the difference is equal to 0.5 kWh/day. The amount of energy saved by using a fuzzy approach is 2 kWh/day which is about 18.7% of the daily load. This is illustrated in Figure 16(c). The comparison study results of the performance indexes show that DC-Bus in the case of the FLC approach is more stable than the deterministic approach. The THDv and frequency deviation in the case of FLC is acceptable while it is not in the case of a deterministic approach. Figure 16(d) shows the comparison study results of the performance indexes.

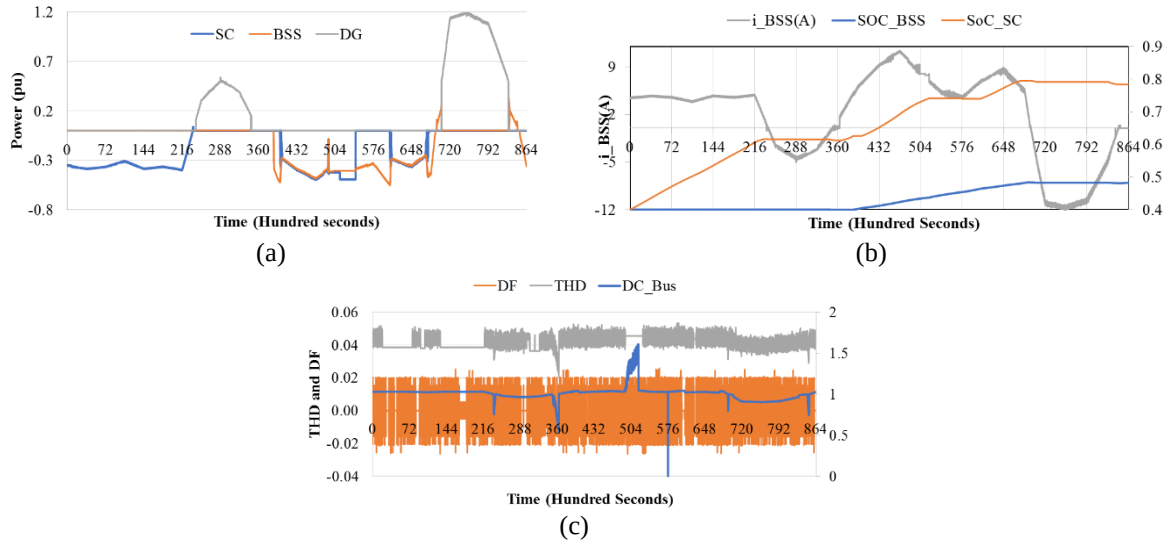

Figure 15. Results of simulation set 2: (a) Injected/absorbed power from BSS, SC, and DG, (b) The SoC_BSS, SoC_SC, and controlling current i_BSS, (c) THDv and Δf in addition to the normalized DC-bus voltage

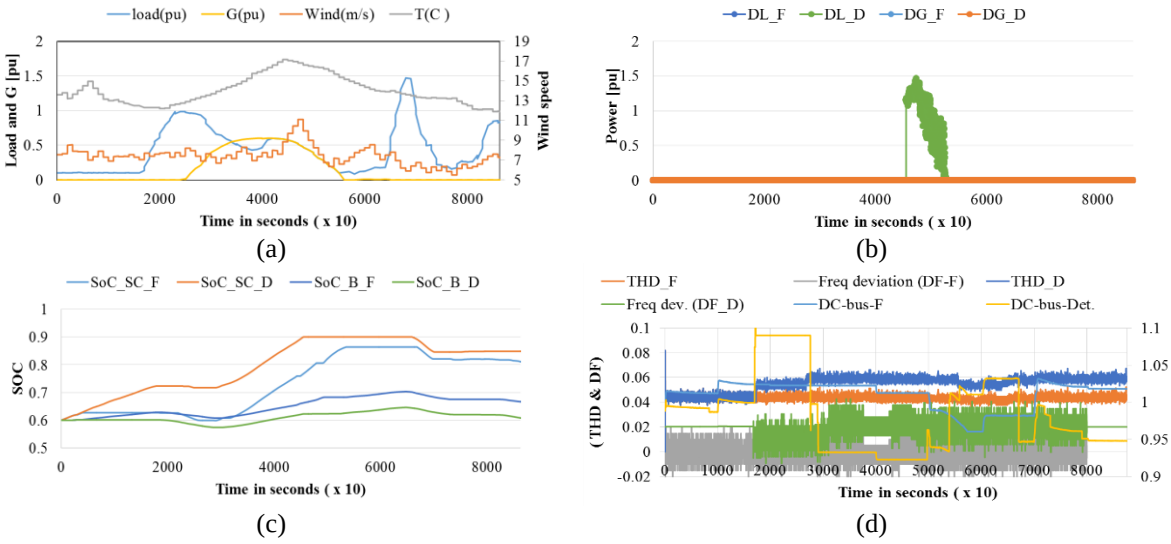

Figure 16. Results of simulation comparison study: (a) Input data of the comparison simulation set, (b) Energy generated from DG and injected to DL, (c) SoC of SC and BSS for both cases: a fuzzy and deterministic approach, (d) DC_Bus, THDv, and frequency deviation for both case

5. CONCLUSION

The results indicate that the FLC-based scheme is capable to adjust the DC bus voltage within assigned limits. A power balancing is confirmed even with the sporadic power output nature of WEG and PVEG. The outcomes approve the efficiency of the suggested power management scheme and are considered as a foundation for practical realization. The outcomes display that DG is effective backup power. The DG can't instantly combine with the DC-bus because of its sluggish dynamic behavior and SC effectively overwhelmed this drawback. The SC also charges and discharges BSS in case of a high shortage and surplus power. The scheme utilizes a dumping load to preserve the stability in the DC-Bus during surplus power cases. This work resolved the low dynamic performance encountered in the conventional approach, lessen steady-state error and switching losses of the power converters. It also lessens THDv of the output voltage signal.

REFERENCES

[1] A. Chahinaze, S. Faquir, and Ali Yahyaouy, "Intelligent Optimization and Management System For Renewable Energy Systems Using Multi-Agent," *IAES International Journal of Artificial Intelligence (IJ-AI),* vol. 8, no. 4, pp. 352-359, 2019.

[2] Von Meier, Alexandra, "Electric power systems: A conceptual introduction," *J. Wiley & Sons,* 2006

[3] Adesanya, Adewale Aremu, and Chelsea Schelly, "Solar PV-diesel hybrid systems for the Nigerian private sector: An impact assessment," *Energy Policy,* vol. 132, pp 196-207, 2019

[4] A. Etxeberria *et al*., "Comparison of three topologies and controls of a hybrid energy storage system for microgrids," *Energy Convers Manage,* vol. 54, no. 1, pp. 113-121, 2012.

[5] Libich, Jiří *et al*., "Supercapacitors: Properties and applications," *J. of Energy Storage,* vol. 17, pp. 224-227, 2018

[6] A. Yasin, M. Alsayed, "Optimization with excess electricity management of a PV, energy storage and diesel generator hybrid system using HOMER Pro software," *International Journal of Applied Power Engineering (IJAPE),* vol. 9, no. 3, pp. 267-283, 2020

[7] M. Sulaiman *et al*., "Course recommendation system using fuzzy logic approach," *Indonesian Journal of Electrical Engineering and Computer Science (IJEECS),* vol. 17, no. 1, pp. 365-371, 2019.

[8] R. Charles *et al*., "Comparison of Mamdani-Type and Sugeno-Type Fuzzy Inference Systems for Transformer Tap Changing System," *International Journal of Advances in Applied Sciences,* vol. 5, no. 4, 2016, Art. no. 163.

[9] Roumila, Zoubir, Djamila Rekioua, and Toufik Rekioua., "Energy management based fuzzy logic controller of hbrid system wind/photovoltaic/diesel with storage battery," *International Journal of Hydrogen Energy,* vol. 42, no. 30, pp. 19525-19535, 2017

[10] Z. Cabrane, Mohammed Ouassaid, and Mohamed Maaroufi, "Battery and supercapacitor for photovoltaic energy storage: A fuzzy logic management," *IET Renew. Power Gener,* vol. 11, no. 8, pp. 1157-1165, 2017

[11] Choudhury, Subhashree *et al*., "A novel control approach based on hybrid Fuzzy Logic and Seeker Optimization for optimal energy management between micro-sources and supercapacitor in an islanded Microgrid," *Journal of King Saud University-Engineering Sciences,* vol. 32, no. 1, pp. 27-41, 2020

[12] Arcos-Aviles, Diego *et al*., "Fuzzy logic-based energy management system design for residential grid-connected microgrids," *IEEE Transactions on Smart Grid,* vol. 9, no. 2, pp. 530-543, 2016

[13] C. Fathia *et al*., "Fuzzy logic energy management for a PV solar home," *En. Procedia,* vol. 134, pp. 723-730, 2017.

[14] Rai, Neerparaj, and Bijay Rai, "Control of fuzzy logic based PV-battery hybrid system for stand-alone DC applications," *Journal of Electrical Systems and Information Technology,* vol. 5, no. 2, pp. 135-143, 2018.

[15] A. Issam, T. Bahi, and H. Bouzeria., "Energy management strategy based on fuzzy logic for compound RES/ESS used in stand-alone application," *International Journal of Hydrogen Energy,* vol. 41, no. 38, pp. 16705-16717, 2016

[16] C. Houssem *et al*., "Fuzzy optimization of a centralized energy management strategy for a hybrid PV/PEMFC system feeding a water pumping station," *International Journal of Renewable Energy Research (IJRER),* vol. 8, no. 4, pp. 2190-2198, 2018

[17] Das, Somnath, and A. Akella, "Power flow control of PV-wind-battery hybrid renewable energy systems for stand-alone application," *International Journal of Renewable Energy Research (IJRER),* vol. 8, no. 1, pp. 36-43, 2018.

[18] M. Jafari *et al*., "Development of a Fuzzy-Logic-Based Energy Management System for a Multiport Multioperation Mode Residential Smart Microgrid," *IEEE Transactions on Power Electronics,* vol. 34, no. 4, pp. 3283-3301, Apr. 2019.

[19] Zahedi, R., and M. M. Ardehali, "Power management for storage mechanisms including battery, SC, and hydrogen of aut. hybrid green power system utilizing multiple optimally-designed FL controllers," *Energy,* vol. 204, 2020, Art. no. 117935.

[20] F. Zhou *et al*., "Energy Management Strategy of Microgrid Based on FL," *2018 2nd IEEE Advanced Information Management, Communicates, Electronic and Automation Control Conference (IMCEC),* 2018.

[21] C. Lebrón *et al*., "An intelligent Battery management system for home Microgrids," *2016 IEEE Power & Energy Society Innovative Smart Grid Technologies Conference (ISGT),* Minneapolis, MN, 2016, pp. 1-5.

[22] Manickavasagam, Krishnan, Naveen Kumar Thotakanama, and Vineetha Puttaraj, "Intelligent energy management system for RE driven ship," in *IET Electrical Systems in Transportation,* vol. 9, no. 1, pp. 24-34, 2019.

[23] J. C. Peña-Aguirre *et. al.,* "Fuzzy Logic Power Management Strategy for a Residential DC-Microgrid," in *IEEE Access,* vol. 8, pp. 116733-116743, 2020.

[24] D. Sera, Remus Teodorescu, and Pedro Rodriguez, "PV panel model based on datasheet values," *IEEE International Symposium on Industrial Electronics*, ISIE 2007, pp. 2392-2396, 2007
[25] M. Masoum, Hooman Dehbonei, and Ewald F. Fuchs, "Theoretical and experimental analyses of PV systems with voltage and current-based maximum power-point tracking," *IEEE Transactions on Energy Conversion*, vol. 17, no. 4, pp. 514-522, 2002.
[26] E. Muljadi *et al*., "Analysis of permanent magnet generator for wind power battery charging," in *Proc. IEEE Industry Applications Conference*, 1996, pp. 541-548.
[27] Manwell J. F., J. G. McGowan and A. L. Rogers, "Wind Energy Explained," *Wiley*, 2003.
[28] C. Krause P.C *et al*., "Analysis of Electric Machinery and drive systems," *2nd ed., IEEE Press*, 2002
[29] S. Benhamed *et al*. "Dynamic modeling of a diesel generator based on electrical and mechanical aspects," *IEEE Electrical Power and Energy Conference (EPEC)*, 2016.
[30] Mathworks, Inc., "generic engine," 2019. [Online], Available: www.mathworks.com/help/ physmod /sdl/ ref/ genericengine.html
[31] Tremblay, O., L.-A. Dessaint, "Experimental Validation of a Battery Dynamic Model for EV Applications," *World Electric Vehicle Journal*, vol. 3, no. 2, pp. 289-298, 2009.
[32] N. Xu and J. Riley, "Nonlinear analysis of a classical system: The double-layer capacitor," *Electrochemistry Communications*, vol. 13, no. 10, pp. 1077-1081, 2011.
[33] A. Yasin, "Distributed Generation Systems Based on Hybrid Wind/PV/FC Structures," PhD thesis, UNICT, 2012.
[34] Mamdani, E.H. and S. Assilian, "An experiment in linguistic synthesis with a fuzzy logic controller," *International Journal of Man-Machine Studies*, vol. 7, no. 1, pp. 1-13, 1975.

BIOGRAPHIES OF AUTHORS

Aysar Yasin is an assistant professor at An-najah National University (ANU), Palestine. He finished his bachelor's degree in electrical engineering from ANU in 1999, master's degree in clean energy and energy conservation engineering from ANU in 2008, and Ph.D. in energy in 2012 from the University of Catania, Italy. His main research interests in distributed energy systems based on renewable energy sources mainly PV and wind energy systems with different types of energy storage systems.

Mohammed Alsayed is an assistant professor at An-najah National University (ANU), Palestine. He finished his bachelor's degree in industrial engineering from ANU in 2005, master degree in clean energy and energy conservation engineering from ANU in 2008, and Ph.D. in energy management in 2013 from the University of Catania, Italy. Alsayed research interests include optimization, energy efficiency, sustainability, waste to energy, and life cycle assessment.